Available online at www.sciencedirect.com
ScienceDirect
International Journal of Engineering Science 45 (2007) 364–380
International Journal of Engineering Science
www.elsevier.com/locate/ijengsci

Free vibration analysis of uniform and stepped cracked beams with circular cross sections

Murat Kisa [a,*], M. Arif Gurel [b]

[a] Department of Mechanical Engineering, Faculty of Engineering, Harran University, Sanliurfa 63300, Turkey
[b] Department of Civil Engineering, Faculty of Engineering, Harran University, Sanliurfa 63300, Turkey

Received 13 February 2007; accepted 29 March 2007
Available online 22 May 2007

Abstract

This paper presents a novel numerical technique applicable to analyse the free vibration analysis of uniform and stepped cracked beams with circular cross section. In this approach in which the finite element and component mode synthesis methods are used together, the beam is detached into parts from the crack section. These substructures are joined by using the flexibility matrices taking into account the interaction forces derived by virtue of fracture mechanics theory as the inverse of the compliance matrix found with the appropriate stress intensity factors and strain energy release rate expressions. To reveal the accuracy and effectiveness of the offered method, a number of numerical examples are given for free vibration analysis of beams with transverse non-propagating open cracks. Numerical results showing good agreement with the results of other available studies, address the effects of the location and depth of the cracks on the natural frequencies and mode shapes of the cracked beams. Modal characteristics of a cracked beam can be employed in the crack recognition process. The outcomes of the study verified that presented method is appropriate for the vibration analysis of uniform and stepped cracked beams with circular cross section.

Keywords: Free vibration; Crack; Stepped beams; Finite element analysis

1. Introduction

Many engineering structures may have structural defects such as cracks due to long-term service, mechanical vibrations, applied cyclic loads etc. Numerous techniques, such as non-destructive monitoring tests, can be used to screen the condition of a structure. Novel techniques to inspect structural defects should be explored. A crack in a structural element modifies its stiffness and damping properties and accordingly influences its dynamical performance. In view of that, the natural frequencies and mode shapes of the structure hold

* Corresponding author. Tel.: +90 533 4524865; fax: +90 414 3440031.
E-mail addresses: mkisa@harran.edu.tr (M. Kisa), agurel@harran.edu.tr (M. Arif Gurel).

0020-7225/$ - see front matter © 2007 Elsevier Ltd. All rights reserved.
doi:10.1016/j.ijengsci.2007.03.014

information relating to the place and dimension of the damage. Vibration analysis allowing online inspection is an attractive method to detect cracks in the structures. Investigation of dynamic behaviour of cracked structures has attracted the attention of several researchers in recent years (Cawley and Adams [1], Gounaris and Dimarogonas [2], Krawczuk and Ostachowicz [3], Ruotolo et al., [4], Kisa et al. [5], Shifrin and Ruotolo [6], Kisa and Brandon [7,8], Viola et al. [9], Krawczuk [10], Patil and Maiti [11], Kisa [12], Kisa and Gurel [13]). Gudmundson [14] investigated the influence of small cracks on the natural frequencies of slender structures by perturbation method as well as by transfer matrix approach. Yuen [15] proposed a methodical finite element procedure to establish the relationship between damage location, damage size and the corresponding modification in the eigen parameters of a cantilever beam. Rizos et al. [16] represented the crack as a massless rotational spring, whose stiffness was calculated by employing fracture mechanics.

There are numerous studies on the vibration analysis of cracked beams with circular cross section and shafts. Dimarogonas and Papadopoulos [17], by using the theory of cracked shafts with dissimilar moments of inertia, investigated the vibration of cracked shafts in bending. Papadopoulos and Dimarogonas [18] studied the free vibration of shafts and presented the influence of the crack on the vibration behaviour of the shafts. Kikidis and Papadopoulos [19] analysed the influence of the slenderness ratio of a non-rotating cracked shaft on the dynamic characteristics of the structure. Zheng and Fan [20] studied the vibration and stability of cracked hollow-sectional beams. Dong et al. [21] presented a continuous model for vibration analysis and parameter identification of a non-rotating rotor with an open crack. They assumed that the cracked rotor was an Euler–Bernoulli beam with circular cross section.

Studies on the vibration of stepped beams are carried out by a number of researchers. Jang and Bert [22] presented the exact and numerical solutions for fundamental natural frequencies of stepped beams for various boundary conditions. Wang [23] analysed the vibration of stepped beams on elastic foundations. Based on an elemental dynamic flexibility method, Lee and Bergman [24] studied the vibration of stepped beams and rectangular plates. In their study, the structure with discontinues was divided into elemental substructures and the displacement field for each was obtained in terms of its dynamic Green's function. Lee and Ng [25] computed the fundamental frequencies and critical buckling loads of simply supported stepped beams by using two algorithms based on the Rayleigh–Ritz method. Rosa et al. [26] performed the free vibration analysis of stepped beams with intermediate elastic supports. Naguleswaran [27] analysed the vibration and stability of an Euler–Bernoulli stepped beam with an axial force.

There are few studies on the vibration of stepped beams with cracks. Employing the transfer matrix method, Tsai and Wang [28] analysed the dynamic characteristics of a stepped shaft and a multi-disc shaft. Nandwana and Maiti [29] presented a method based on measurement of natural frequencies for detection of the location and size of a crack in a stepped cantilever beam. Chaudhari and Maiti [30] presented an experimentally verified method for prediction of location and size of crack in stepped beams with cracks. Li [31,32] analysed the vibratory characteristics of multi-step beams with an arbitrary number of cracks and concentrated masses.

Abraham and Brandon [33] and Brandon and Abraham [34] presented a method utilising substructure normal modes to predict the vibration properties of a cantilever beam with a closing crack. The full eigensolution of a structure containing substructures each having large numbers of degrees of freedom can be costly in computing time. A method known as component mode synthesis or substructure technique, proposed by Hurty [35], made possible the problem to be broken up into separate elements and thus considerably reduced its complexity. The component mode synthesis method was initially developed to ease the study of very large structures but in this study it is used for another purpose. The advantage of the method in the case of a non-linear cracked beam stems from the fact that, when a beam is split into components at the crack section, each substructure becomes linear and analytical or numerical results are available for their normal modes. Consequently, the initial non-linear system with local discontinuities in stiffness at the crack sections is now composed of linear segments. An important characteristic of the model developed in this study is that it allows discontinuity in the displacement field at the crack section when the crack is open. The substructures are connected by an artificial and massless spring whose stiffness coefficients are functions of the compliance coefficients. To the best of the authors' knowledge, the presented method is applied for the first time to the uniform and stepped cracked beams of circular cross section which commonly used in engineering structures.

2. Theoretical model

The model chosen is a stepped cantilever beam of length L and diameters D_1 ($D_1 = 2R_1$) and D_2 ($D_2 = 2R_2$), having a transverse open edge crack of depth a at a variable position L_1 (Fig. 1). Length of the first part is αL in which α can be chosen between 0 and 1.

The beam is divided into two components at the crack section leading to a substructure approach. Accordingly, as mentioned before, the global non-linear system with a local stiffness discontinuity is detached into two linear subsystems. Each part is also divided into finite elements with two nodes and three degrees of freedom at each node as shown in Fig. 2.

2.1. Local flexibility matrix of a cracked beam with circular cross section

As a result of the strain energy concentration at the surrounding area of the crack tip, the existence of cracks in structures is a resource of local flexibility which subsequently influences the dynamic performance of the structures. These flexibility coefficients are expressed by stress intensity factors derived through Castigliano's theorem in the linear elastic range. The strain energy release rate, J, represents the elastic energy in relation to a unit increase in length ahead of the crack front. For plane strain, J can be given as (Irwin [36])

$$J = \frac{1-v^2}{E}K_{\mathrm{I}}^2 + \frac{1-v^2}{E}K_{\mathrm{II}}^2 + \frac{1+v}{E}K_{\mathrm{III}}^2 \tag{1}$$

where v, E, K_{I}, K_{II} and K_{III} are Poisson's ratio, modulus of elasticity, and the stress intensity factors for the mode I, II and III deformation types, respectively. As torsional effects will not be concerned about in this study, simply mode I and mode II types of deformations are considered. The superposition of the stress intensity factors gives, for the strain energy release rate, the subsequent expression

$$J = \frac{1-v^2}{E^*}\left\{\left(K_{\mathrm{I}}(P_1) + K_{\mathrm{I}}(P_3)\right)^2 + K_{\mathrm{II}}(P_2)^2\right\} \tag{2}$$

where P_1, P_2 and P_3 are the axial force, shear force and bending moment, respectively, Fig. 2. $E^* = E$ for plane strain and $E^* = E/(1-v^2)$ for plane stress. Bending moment P_3 and the axial force P_1 make the contribution

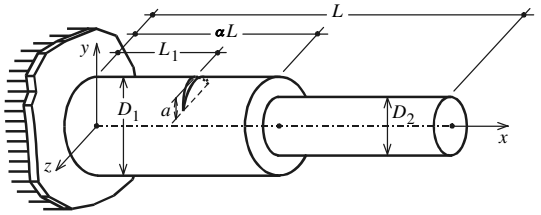

Fig. 1. Geometry of the stepped cantilever beam with a crack.

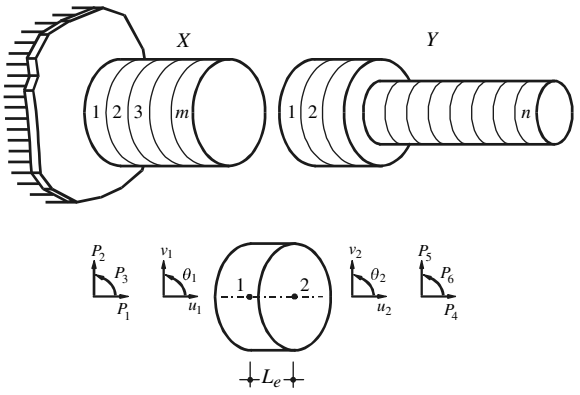

Fig. 2. Components of cracked beam and their finite element model.

to the opening mode, mode I. The edge sliding mode, mode II, receives a contribution from the shear force P_2. $K_{\mathrm{I}}(P_1)$, $K_{\mathrm{I}}(P_3)$ and $K_{\mathrm{II}}(P_2)$ can be written as follow (Tada et al. [37])

$$K_{\mathrm{I1}} = \frac{P_1}{\pi R^2}\sqrt{\pi a}F_1\left(\frac{a}{h_x}\right) \tag{3}$$

where

$$F_1\left(\frac{a}{h_x}\right) = \sqrt{\frac{2h_x}{\pi a}tg\left(\frac{\pi a}{2h_x}\right)}\frac{0.752 + 2.02\left(\frac{a}{h_x}\right) + 0.37\left(1 - \sin\frac{\pi a}{2h_x}\right)^3}{\cos\left(\frac{\pi a}{2h_x}\right)} \tag{4}$$

$$K_{\mathrm{I3}} = \frac{4P_3}{\pi R^4}\sqrt{\pi a}F_2\left(\frac{a}{h_x}\right) \tag{5}$$

where

$$F_2\left(\frac{a}{h_x}\right) = \sqrt{\frac{2h_x}{\pi a}tg\left(\frac{\pi a}{2h_x}\right)}\frac{0.923 + 0.199\left(1 - \sin\frac{\pi a}{2h_x}\right)^4}{\cos\left(\frac{\pi a}{2h_x}\right)} \tag{6}$$

$$K_{\mathrm{II2}} = \frac{\kappa P_2}{\pi R^2}\sqrt{\pi a}F_3\left(\frac{a}{h_x}\right) \tag{7}$$

where

$$F_3\left(\frac{a}{h_x}\right) = \frac{1.122 - 0.561\left(\frac{a}{h_x}\right) + 0.085\left(\frac{a}{h_x}\right)^2 + 0.180\left(\frac{a}{h_x}\right)^3}{\sqrt{1 - \frac{a}{h_x}}} \tag{8}$$

where the coefficient κ is a numerical factor depending on the shape of the cross section and derived from Timoshenko beam theory (Cowper [38]), a is the crack depth and h_x is the height of the strip, Fig. 3, and written as

$$h_x = 2\sqrt{R^2 - x^2} \tag{9}$$

where R is the radius of the cross section of the beam.

If the stress intensity expressions are substituted into Eq. (2), the next expression is obtained

$$J(a) = \frac{1 - \nu^2}{E^*}\pi a\left\{\begin{array}{l}\frac{P_1^2}{\pi^2 R^4}F_1^2\left(\frac{a}{h_x}\right) + \frac{16P_3^2}{\pi^2 R^8}(R^2 - x^2)F_3^2\left(\frac{a}{h_x}\right) + \frac{8P_1P_3}{\pi^2 R^6}\sqrt{R^2 - x^2}F_1\left(\frac{a}{h_x}\right)F_3\left(\frac{a}{h_x}\right)\\ + \frac{\kappa^2 P_2^2}{\pi^2 R^4}F_2^2\left(\frac{a}{h_x}\right)\end{array}\right\} \tag{10}$$

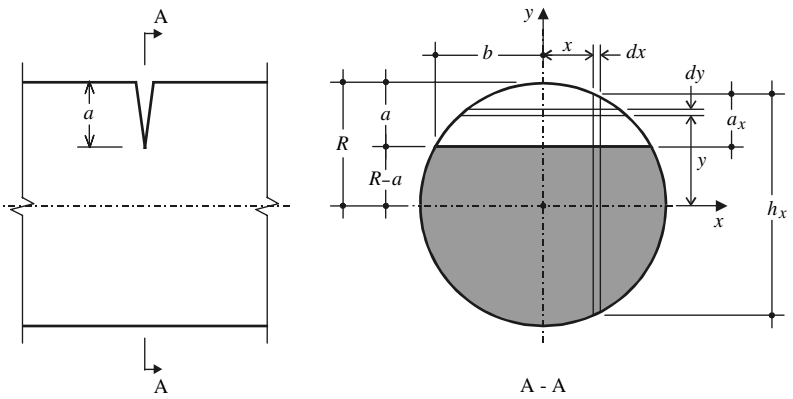

Fig. 3. The geometry of the cracked circular cross section.

If U is the strain energy of a cracked structure with a crack area A under the load P_i, then the relation between J and U is

$$J = \frac{\partial U(P_i, A)}{\partial A} \tag{11}$$

In accordance with the Castigliano's theorem, the additional displacement caused by the crack in the direction of P_i can be given as

$$u_i = \frac{\partial U(P_i, A)}{\partial P_i} \tag{12}$$

Substituting Eq. (11) into Eq. (12) gives the final expression between displacement and strain energy release rate J as

$$u_i = \frac{\partial}{\partial P_i} \int_A J(P_i, A) \mathrm{d}A \tag{13}$$

Now, the flexibility coefficients which are the functions of the crack shape and the stress intensity factors can be introduced as follows (Dimarogonas and Paipetis [39])

$$c_{ij} = \frac{\partial u_i}{\partial P_j} = \frac{\partial^2}{\partial P_i \partial P_j} \int_A J(P_i, A) \mathrm{d}A \tag{14}$$

Finally, the flexibility coefficients c_{11}, c_{13}, c_{22} and c_{33} are obtained as

$$c_{11} = \frac{2}{E^* \pi R^4} \int_{-b}^{b} \int_0^{a_x} y F_1^2 \left(\frac{a}{h_x}\right) \mathrm{d}y \, \mathrm{d}x \tag{15}$$

$$c_{13} = \frac{8}{E^* \pi R^6} \int_{-b}^{b} \int_0^{a_x} y \sqrt{R^2 - x^2} F_1 \left(\frac{a}{h_x}\right) F_3 \left(\frac{a}{h_x}\right) \mathrm{d}y \, \mathrm{d}x \tag{16}$$

$$c_{22} = \frac{2\kappa^2}{E^* \pi R^4} \int_{-b}^{b} \int_0^{a_x} y F_2^2 \left(\frac{a}{h_x}\right) \mathrm{d}y \, \mathrm{d}x \tag{17}$$

$$c_{33} = \frac{32}{E^* \pi R^8} \int_{-b}^{b} \int_0^{a_x} y (R^2 - x^2) F_3^2 \left(\frac{a}{h_x}\right) \mathrm{d}y \, \mathrm{d}x \tag{18}$$

where b and a_x are the boundary of the strip and the local crack depth, Fig. 3, respectively, and given as

$$\begin{aligned} b &= \sqrt{R^2 - (R - a)^2} \\ a_x &= \sqrt{R^2 - x^2} - (R - a) \end{aligned} \tag{19}$$

Dimensionless flexibility coefficients are calculated numerically along with the subsequent expressions and drawn in Fig. 4.

$$\begin{aligned} c_{11}^* &= E^* \pi R c_{11} \quad c_{13}^* = E^* \pi R^2 c_{13} \\ c_{22}^* &= \frac{E^* \pi R c_{22}}{\kappa^2} \quad c_{33}^* = E^* \pi R^3 c_{33} \end{aligned} \tag{20}$$

Since the shear force does not contribute to the opening mode of the crack, the compliance matrix, in relation to displacement vector $\delta(u, v, \theta)$, can be written as

$$C = \begin{bmatrix} c_{11} & 0 & c_{13} \\ 0 & c_{22} & 0 \\ c_{31} & 0 & c_{33} \end{bmatrix}_{(3\times 3)} \tag{21}$$

The inverse of the compliance matrix C^{-1} is the stiffness matrix of the nodal point and given as

$$K_{\mathrm{cr}} = C^{-1} \tag{22}$$

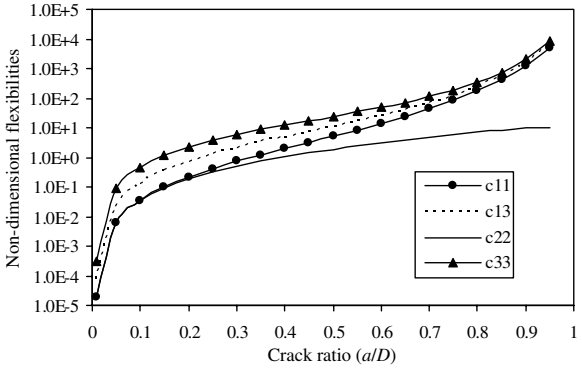

Fig. 4. Non-dimensional compliance coefficients as a function of the crack depth ratio a/D.

2.2. Coupling of the substructures by springs

Consider two undamped components X and Y joined together by means of springs capable of carrying axial, shearing and bending effects, Fig. 5. For this system the equation of motion, in matrix notation, is given as

$$\begin{bmatrix} M_X & 0 \\ 0 & M_Y \end{bmatrix} \begin{Bmatrix} \ddot{q}_X \\ \ddot{q}_Y \end{Bmatrix} + \begin{bmatrix} K_X & 0 \\ 0 & K_Y \end{bmatrix} \begin{Bmatrix} q_X \\ q_Y \end{Bmatrix} = \begin{Bmatrix} f_X(t) \\ f_Y(t) \end{Bmatrix} \tag{23}$$

where q and $f(t)$ are the generalised displacement and external force vector, respectively. M_X, M_Y and K_X, K_Y are mass and stiffness matrices for the components X and Y, respectively. Mass and stiffness matrices are taken from the paper of Friedman and Kosmatka [40]. Eq. (23) gives the eigenvalue equation as

$$\left(\begin{bmatrix} K_X & 0 \\ 0 & K_Y \end{bmatrix} - \begin{bmatrix} \omega_X^2 & 0 \\ 0 & \omega_Y^2 \end{bmatrix} \begin{bmatrix} M_X & 0 \\ 0 & M_Y \end{bmatrix} \right) \begin{Bmatrix} q_X \\ q_Y \end{Bmatrix} = \begin{Bmatrix} 0 \\ 0 \end{Bmatrix} \tag{24}$$

Eq. (24) gives eigenvalues and modal matrix for the components X and Y.

On a particular spring, the exerted forces, F_X and F_Y, are given by

$$\begin{aligned} F_X &= K(q_X - q_Y) \\ F_Y &= K(q_Y - q_X) \end{aligned} \tag{25}$$

where q_X and q_Y are the displacements of the connection points, Fig. 5. Then Eq. (25) can be written as

$$\begin{Bmatrix} F_X \\ F_Y \end{Bmatrix} = K_C \begin{Bmatrix} q_X \\ q_Y \end{Bmatrix} \tag{26}$$

where K_C is the connection matrix and given as

$$K_C = \begin{bmatrix} K_{cr}^{-1} & -K_{cr}^{-1} \\ -K_{cr}^{-1} & K_{cr}^{-1} \end{bmatrix} \tag{27}$$

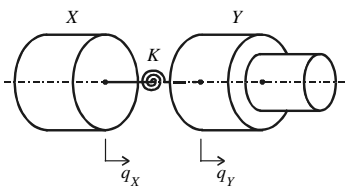

Fig. 5. System of the components connected by spring.

where K_{cr} is the stiffness matrix of the nodal point and given by Eq. (22). The force vector $f(t)$ comprises applied forces $g(t)$ and forces resulting from the springs $d(t)$, such that

$$f(t) = g(t) + d(t) \tag{28}$$

From the equilibrium

$$d(t) = -\begin{Bmatrix} F_X \\ F_Y \end{Bmatrix} = -K_C \begin{Bmatrix} q_X \\ q_Y \end{Bmatrix} \tag{29}$$

Substituting Eqs. (28) and (29) into Eq. (23) gives

$$\begin{bmatrix} M_X & 0 \\ 0 & M_Y \end{bmatrix} \begin{Bmatrix} \ddot{q}_X \\ \ddot{q}_Y \end{Bmatrix} + \begin{bmatrix} K_X & 0 \\ 0 & K_Y \end{bmatrix} \begin{Bmatrix} q_X \\ q_Y \end{Bmatrix} = -[K_C] \begin{Bmatrix} q_X \\ q_Y \end{Bmatrix} + \begin{Bmatrix} g_X(t) \\ g_Y(t) \end{Bmatrix} \tag{30}$$

or

$$\begin{bmatrix} M_X & 0 \\ 0 & M_Y \end{bmatrix} \begin{Bmatrix} \ddot{q}_X \\ \ddot{q}_Y \end{Bmatrix} + \left(\begin{bmatrix} K_X & 0 \\ 0 & K_Y \end{bmatrix} + [K_C] \right) \begin{Bmatrix} q_X \\ q_Y \end{Bmatrix} = \begin{Bmatrix} g_X(t) \\ g_Y(t) \end{Bmatrix} \tag{31}$$

If modal vector ϕ_{ij} is normalised by the mass, the following expression is given

$$\psi_{ij} = \frac{\phi_{ij}}{\sqrt{m_{jj}}} \tag{32}$$

where ψ_{ij} is mass normalised mode vector. By using the transformation

$$\begin{Bmatrix} q_X \\ q_Y \end{Bmatrix} = \begin{bmatrix} \psi_X & 0 \\ 0 & \psi_Y \end{bmatrix} \begin{Bmatrix} s_X \\ s_Y \end{Bmatrix}^T \tag{33}$$

where s_X and s_Y are the principal coordinate vectors. By premultiplying ψ^T and substituting Eqs. (32) and (33) into Eq. (31), gives

$$I \begin{Bmatrix} \ddot{s}_X \\ \ddot{s}_Y \end{Bmatrix} + \begin{bmatrix} \omega_X^2 & 0 \\ 0 & \omega_Y^2 \end{bmatrix} \begin{Bmatrix} s_X \\ s_Y \end{Bmatrix} + \begin{bmatrix} \psi_X & 0 \\ 0 & \psi_Y \end{bmatrix}^T [K_C] \begin{bmatrix} \psi_X & 0 \\ 0 & \psi_Y \end{bmatrix} \begin{Bmatrix} s_X \\ s_Y \end{Bmatrix} = \begin{bmatrix} \psi_X & 0 \\ 0 & \psi_Y \end{bmatrix}^T \begin{Bmatrix} g_X(t) \\ g_Y(t) \end{Bmatrix} \tag{34}$$

where

$$\begin{aligned} I &= \psi_X^T M_X \psi_X = \psi_Y^T M_Y \psi_Y \\ \omega_X^2 &= \psi_X^T K_X \psi_X \\ \omega_Y^2 &= \psi_Y^T K_Y \psi_Y \end{aligned} \tag{35}$$

Eq. (34), for free vibration, gives the eigenvalue equation as

$$\left(\begin{bmatrix} \omega_X^2 & 0 \\ 0 & \omega_Y^2 \end{bmatrix} + \begin{bmatrix} \psi_X^T & 0 \\ 0 & \psi_Y^T \end{bmatrix} [K_C] \begin{bmatrix} \psi_X & 0 \\ 0 & \psi_Y \end{bmatrix} - \omega^2 \begin{bmatrix} I & 0 \\ 0 & I \end{bmatrix} \right) \begin{Bmatrix} s_X \\ s_Y \end{Bmatrix} = \{0\} \tag{36}$$

From Eq. (36) the eigenvalues and eigenvectors of the system can be determined. After solving this equation, the displacements for each component are calculated by using Eq. (33).

3. Numerical examples and discussion

3.1. Uniform cantilever beam with a crack

Presented method, initially, has been applied to a uniform cracked cantilever beam with circular cross section, Fig. 6. The geometrical properties of the beam are length $L = 2$ m, slenderness ratios $R/L = 0.1$, 0.06 and 0.04. Calculation has been performed with the numerical values, Young's modulus $E = 216 \times 10^9$ Nm^{-2}, the Poisson's ratio $v = 0.33$ and mass density $\rho = 7.85 \times 10^3$ kg m^{-3}.

Fig. 7 illustrates the first non-dimensional frequencies of the cracked beam as a function of the crack depth ratio (a/D) for several slenderness ratios R/L (0.1, 0.06 and 0.04). In the analysis, the crack location is chosen as $L_1/L = 0.2$. In this study, non-dimensional natural frequencies are normalised according to next equation

$$\omega = \frac{\omega_{cr}}{\omega_{nc}} \tag{37}$$

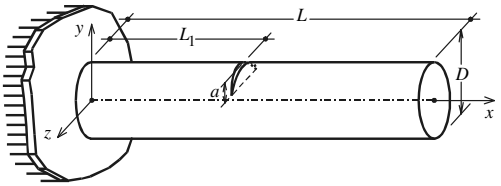

Fig. 6. Geometry of the uniform cantilever beam with a crack.

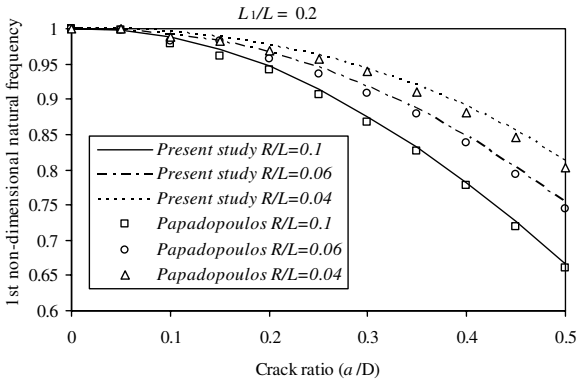

Fig. 7. First non-dimensional natural frequencies as a function of crack depth ratio, for several slenderness ratios $R/L = 0.1, 0.06, 0.04$ and crack position $L_1/L = 0.2$.

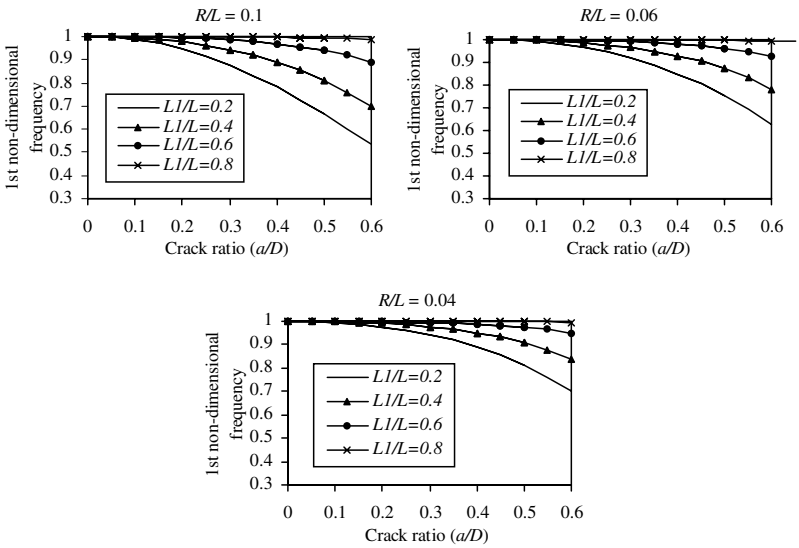

Fig. 8. First non-dimensional natural frequency as a function of crack depth ratio, for several slenderness ratios $R/L = 0.1, 0.06, 0.04$, and crack locations $L_1/L = 0.2, 0.4, 0.6$, and 0.8.

where ω_{cr} and ω_{nc} refer to the natural frequency of the cracked and non-cracked cantilever beams, respectively.

The natural frequencies of the cracked beam are lower than those of corresponding intact beam, as expected. Differences in the frequencies get higher as the depth of the crack increases. Because of the bending moment along the beam, which is concentrated at the fixed end, a crack closer to the free end will have a smaller effect on the fundamental frequency than a crack closer to the fixed end. It can be obviously seen from the Fig. 7 that when the slenderness ratio (R/L) increases, the frequency reduction gets higher, too. The results obtained by the current approach are compared with those of Papadopoulos and Dimarogonas [41] and as

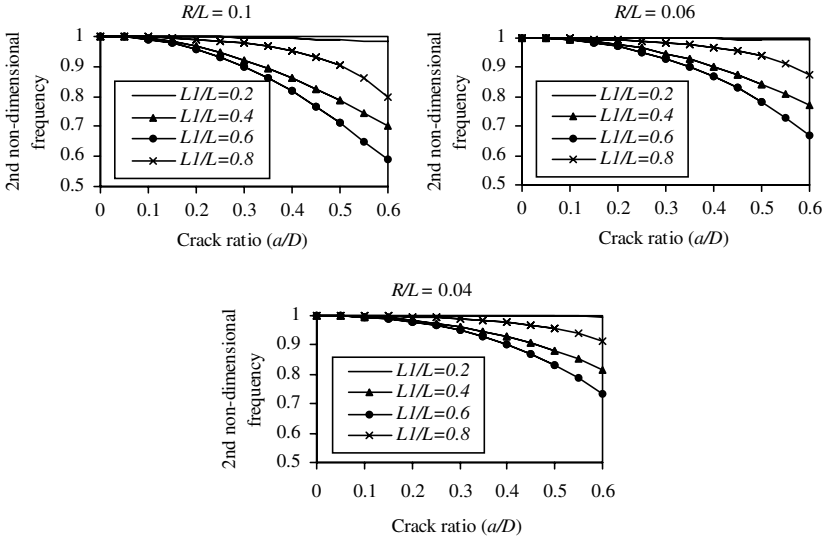

Fig. 9. Second non-dimensional natural frequency as a function of crack depth ratio, for several slenderness ratios $R/L = 0.1, 0.06, 0.04$, and crack locations $L_1/L = 0.2, 0.4, 0.6$, and 0.8.

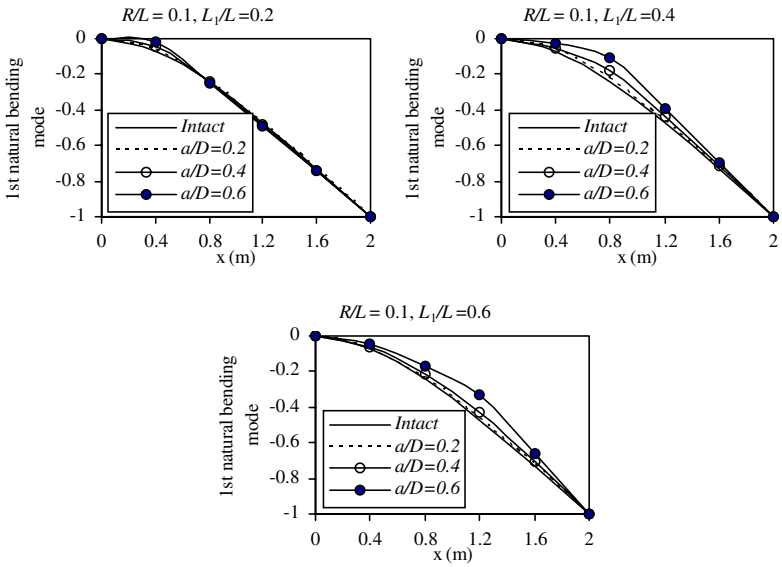

Fig. 10. First natural bending mode as a function of crack depth ratio, for slenderness ratio $R/L = 0.1$, and crack locations $L_1/L = 0.2, 0.4$, and 0.6.

is noticed from the Fig. 7, an excellent concurrence has been found between the results. Figs. 8 and 9 demonstrate the first and second non-dimensional natural frequencies as a function of crack depth ratio for several slenderness ratios $R/L = 0.1, 0.06$, and 0.04, and crack locations $L_1/L = 0.2, 0.4, 0.6$, and 0.8. As perceptible from the figures, the first frequency reduction is higher when the crack location L_1/L is equal to 0.2, while the frequency difference is higher in the second frequency when the crack location L_1/L is between 0.4 and 0.6.

Figs. 10–12 illustrate the first, second and third natural bending mode shapes as a function of crack depth ratio for different slenderness ratios and crack locations $L_1/L = 0.2, 0.4$, and 0.6. From the mode shapes the position of the crack can be clearly seen.

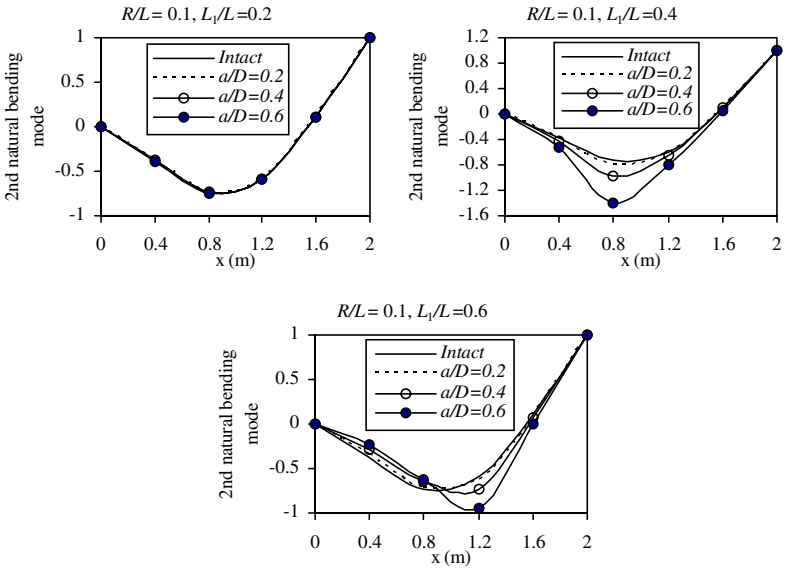

Fig. 11. Second natural bending mode as a function of crack depth ratio, for slenderness ratio $R/L = 0.1$, and crack locations $L_1/L = 0.2, 0.4$, and 0.6.

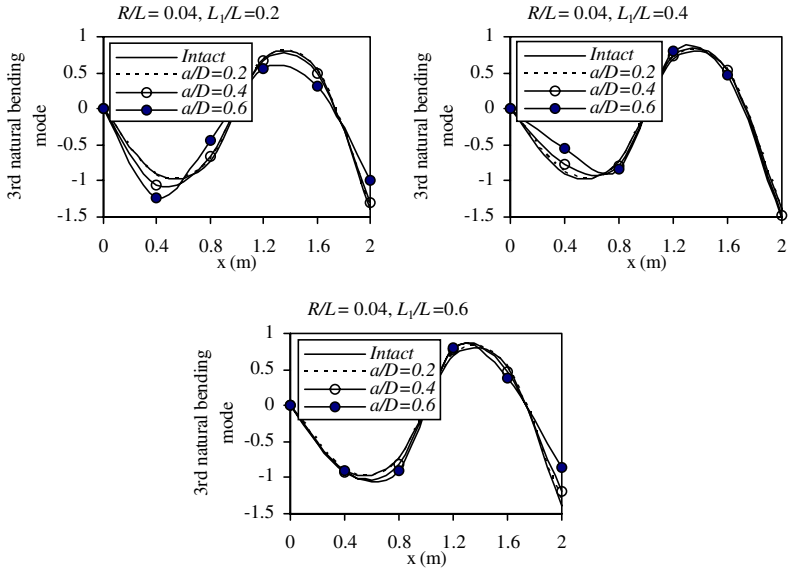

Fig. 12. Third natural bending mode as a function of crack depth ratio, for slenderness ratio $R/L = 0.04$, and crack locations $L_1/L = 0.2, 0.4$, and 0.6.

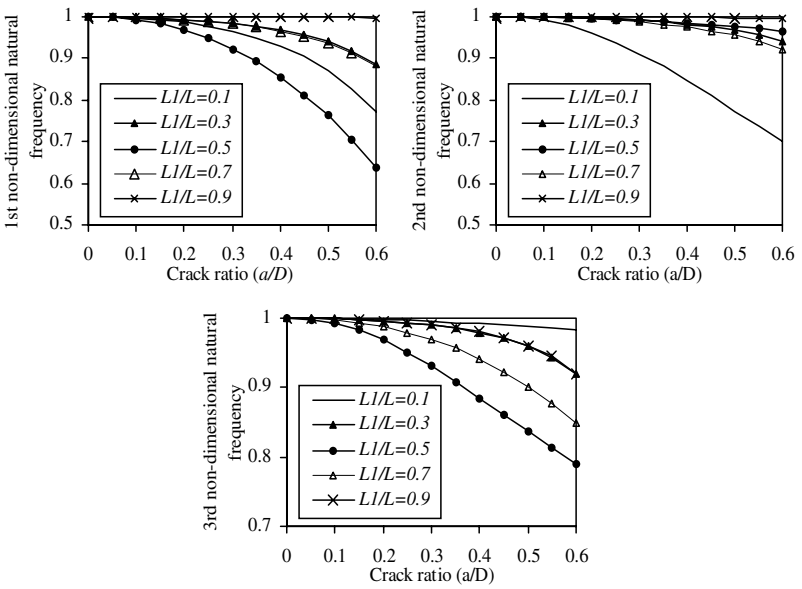

Fig. 13. First, second and third non-dimensional natural frequencies as a function of crack depth ratio for several crack locations $L_1/L = 0.1, 0.3, 0.5, 0.7$, and 0.9.

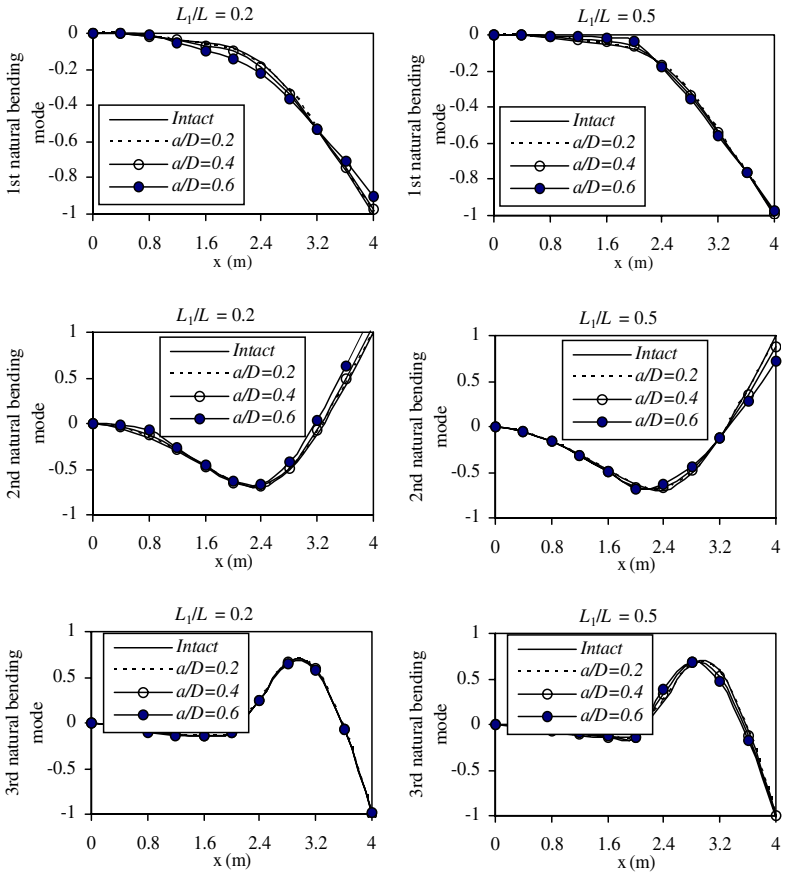

Fig. 14. First, second and third natural bending mode shapes as a function of crack depth ratio for crack locations $L_1/L = 0.2$ and 0.5.

3.2. Stepped cantilever beam with a crack

Second example is selected as a stepped cantilever beam with a crack, Fig. 1. The material properties of the beam for the present and subsequent instances are identical to the beam in the previous example. The length of the beam is $L = 4$ m and the step part is at the middle of the beam ($\alpha = 0.5$). In the first and second parts of the beam the slenderness ratios are chosen as $R_1/L = 0.1$ and $R_2/L = 0.04$, respectively. Fig. 13 displays the first, second and third non-dimensional natural frequencies as a function of crack depth ratio for several crack locations $L_1/L = 0.1, 0.3, 0.5, 0.7$, and 0.9.

From Fig. 13, one can discern that the greater drops in the first and third natural frequencies are occurred when the crack is located just at the step part, $L_1/L = 0.5$, as the stiffness of the beam decreases due to the stepped variation in diameter and the presence of crack. If the crack is located near the fixed end the reduction in the second natural frequencies is the highest. When the first non-dimensional natural frequency is considered, the crack located at the step part of the beam causes more reductions in the natural frequencies compared to a crack situated near to the fixed end.

Fig. 14 illustrates the first, second and third natural bending mode shapes as a function of crack depth ratio for crack locations $L_1/L = 0.2, 0.5$. From the Fig. 14, it can be seen that when the crack is closer to step part of the beam, $L_1/L = 0.5$, the differences in the mode shapes of cracked and intact beams are getting higher. Exploring the mode shapes, it can be observed that at the crack section the deviations of mode shapes of cracked and intact beams are greater. Accordingly, utilising the mode shapes the position of the crack can be detected easily.

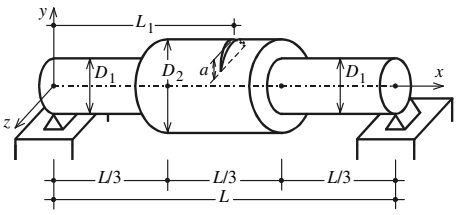

Fig. 15. Geometry of a two-step simply supported beam with a crack.

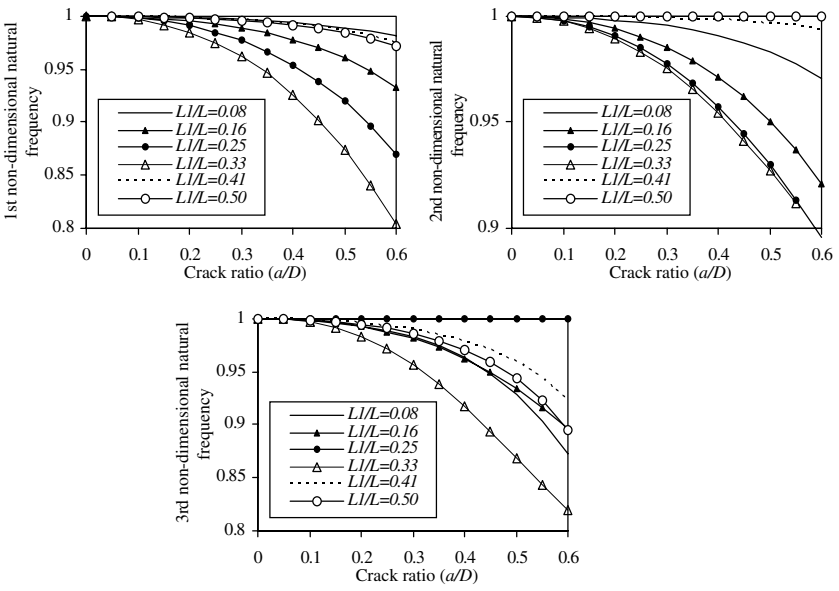

Fig. 16. First, second and third non-dimensional natural frequencies as a function of crack depth ratio for several crack locations $L_1/L = 0.08, 0.16, 0.25, 0.33, 0.41$, and 0.50.

3.3. Two-step simply supported beam with a crack

Third example is selected as a two-step simply supported cracked beam with circular cross section, Fig. 15. The length of the beam is $L = 6$ m and the step locations are at the 1/3 and 2/3 of the beam length. In the first,

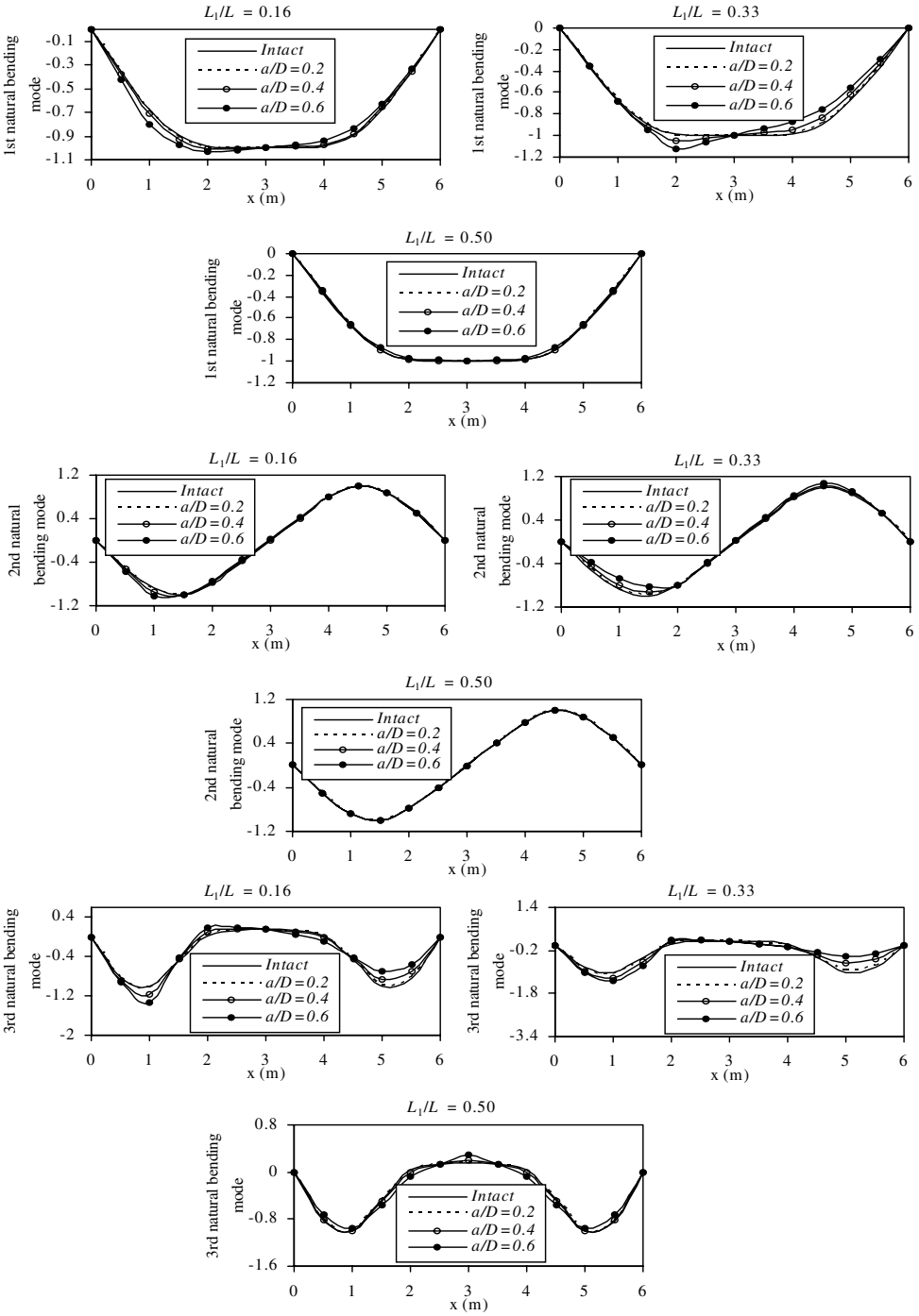

Fig. 17. First, second and third natural bending mode shapes as a function of crack depth ratio for crack locations $L_1/L = 0.16$, 0.33, and 0.50.

second and third parts of the beam, the slenderness ratios are chosen as $R_1/L = 0.04$, $R_2/L = 0.1$ and $R_3/L = 0.04$, respectively.

Fig. 16 demonstrates the first, second and third non-dimensional natural frequencies as a function of crack depth ratio for several crack locations $L_1/L = 0.08, 0.16, 0.25, 0.33, 0.41$ and 0.50. Due to the symmetry, only the results belong to the one half of the beam is shown in this figure. It is clear from the Fig. 16 that the larger falls in the first, second and third natural frequencies are observed when the crack is located at the step, $L_1/L = 0.33$.

Fig. 17 illustrates the first, second and third natural bending mode shapes as a function of crack depth ratio for crack locations $L_1/L = 0.16, 0.33$, and 0.50. Similar to the natural frequencies, the largest changes in the mode shapes of cracked and intact beams occur when a crack is located at the step, Fig. 17.

3.4. Two-step simply supported beam with two cracks

The last example is a two-step simply supported beam with two cracks, Fig. 18. The geometrical properties of the beam are chosen identical to the one given in the former example. In the first, second and third parts of the beam the slenderness ratios are chosen as $R_1/L = 0.04$, $R_2/L = 0.1$ and $R_3/L = 0.04$, respectively.

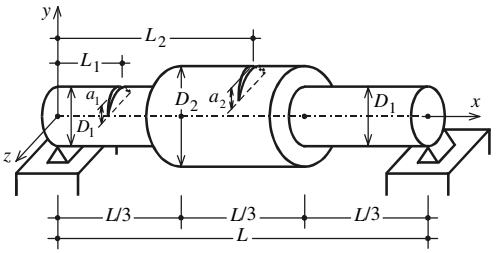

Fig. 18. Geometry of a two-step simply supported beam with two cracks.

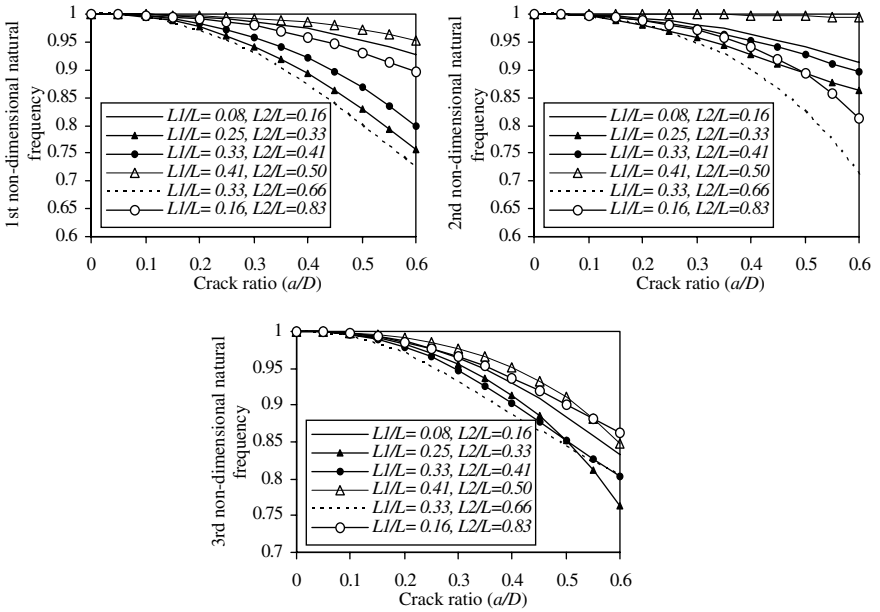

Fig. 19. First, second and third non-dimensional natural frequencies as a function of crack depth ratio for several crack locations $L_1/L = 0.08 - L_2/L = 0.16$, $L_1/L = 0.25 - L_2/L = 0.33$, $L_1/L = 0.33 - L_2/L = 0.41$, $L_1/L = 0.41 - L_2/L = 0.50$, $L_1/L = 0.33 - L_2/L = 0.66$, $L_1/L = 0.16 - L_2/L = 0.83$.

Fig. 19 illustrates the first, second and third non-dimensional natural frequencies as a function of crack depth ratio for several crack locations $L_1/L = 0.08 - L_2/L = 0.16$, $L_1/L = 0.25 - L_2/L = 0.33$, $L_1/L = 0.33 - L_2/L = 0.41$, $L_1/L = 0.41 - L_2/L = 0.50$, $L_1/L = 0.33 - L_2/L = 0.66$, $L_1/L = 0.16 - L_2/L = 0.83$.

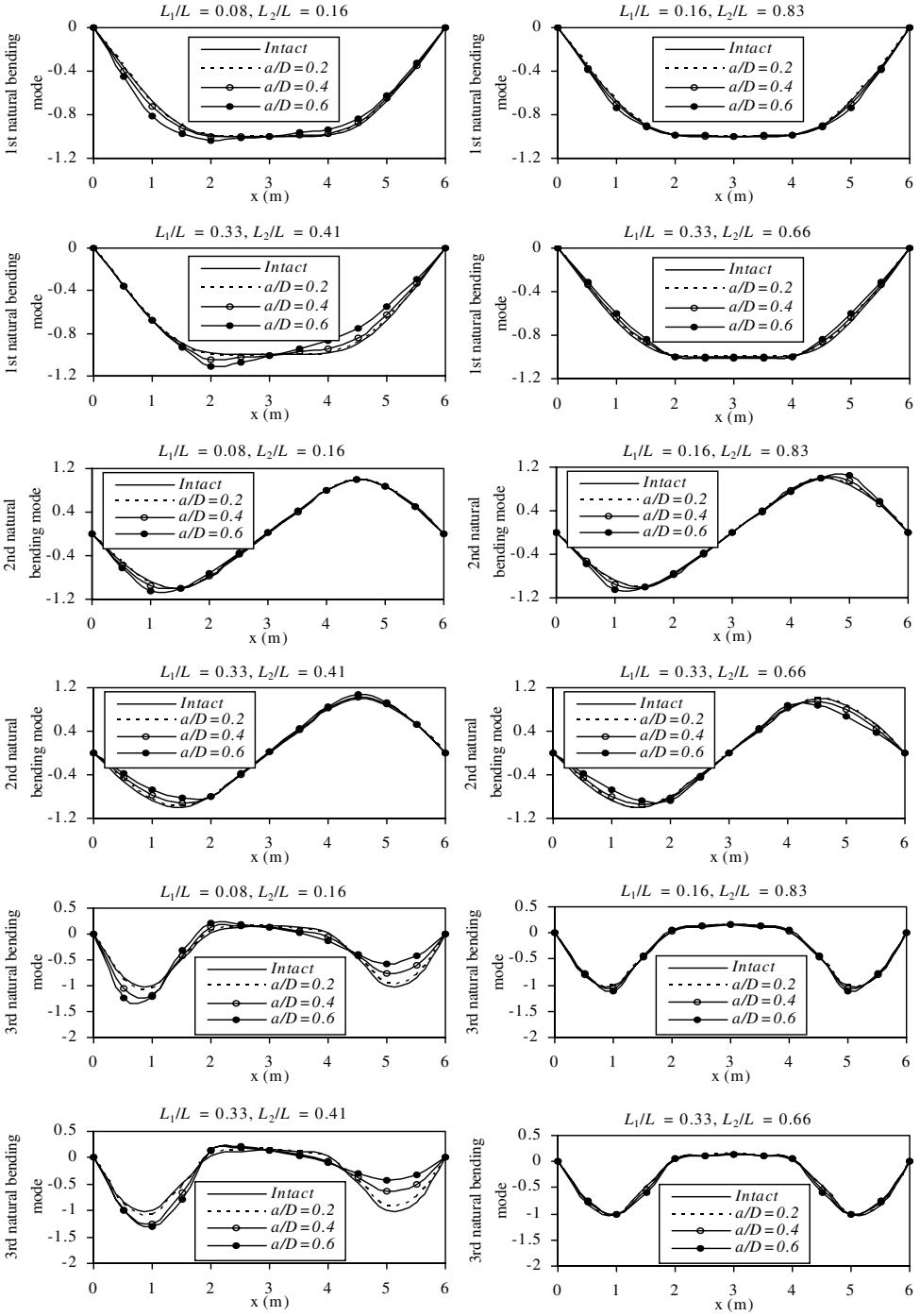

Fig. 20. First, second and third natural bending mode shapes as a function of crack depth ratio for crack locations $L_1/L = 0.08 - L_2/L = 0.16$, $L_1/L = 0.16 - L_2/L = 0.83$, $L_1/L = 0.33 - L_2/L = 0.41$, $L_1/L = 0.33 - L_2/L = 0.66$.

It is clear from the Fig. 19 that the larger decreases in the first, second and third natural frequencies are seen when the cracks are located at the step parts, $L_1/L = 0.33 - L_2/L = 0.66$.

Fig. 20 shows the first, second and third natural bending mode shapes as a function of crack depth ratio for crack locations $L_1/L = 0.08 - L_2/L = 0.16$, $L_1/L = 0.16 - L_2/L = 0.83$, $L_1/L = 0.33 - L_2/L = 0.41$, $L_1/L = 0.33 - L_2/L = 0.66$. From the Fig. 20, the effects of the step parts of the beam where the cracks are located on the mode shapes can be noticed.

4. Conclusions

In this paper a new approach for the vibration analysis of uniform and stepped cracked beams with circular cross sections is presented. In the method, the component mode synthesis technique accompanied by the finite element method is used and a non-linear problem separated into linear subsystems. As the whole structure is detached from the crack section, making use of the present approach is believed to offer an efficient method capable of investigating the non-linear interface effects such as contact and impact that occur when crack closes.

It is revealed that the knowledge of modal data of cracked beams forms an important aspect in assessing the structural failure. Presented four numerical examples verified that the proposed method is effective end versatile. Besides, it is shown that the crack locations and sizes can notably influence the modal features, i.e. natural frequencies and mode shapes, of the cracked beams especially when the cracks are located at the step parts of the beams.

It is evident that, the application of the present study is restricted to the vibration analysis of beams with non-propagating open cracks. Some potential extensions, which are left for future works, of the present study are the investigation of the beams with other cross sections and inclusion of contact and impact effects when the crack breathes.

References

[1] P. Cawley, R.D. Adams, The location of defects in structures from measurements of natural frequencies, J. Strain Anal. 14 (1979) 49–57.
[2] G. Gounaris, A.D. Dimarogonas, A finite element of a cracked prismatic beam for structural analysis, Comput. Struct. 28 (1988) 309–313.
[3] M. Krawczuk, W.M. Ostachowicz, Transverse natural vibrations of a cracked beam loaded with a constant axial force, J. Vib. Acoust. 115 (1993) 524–528.
[4] R. Ruotolo, C. Surace, P. Crespo, D. Storer, Harmonic analysis of the vibrations of a cantilevered beam with a closing crack, Comput. Struct. 61 (1996) 1057–1074.
[5] M. Kisa, J.A. Brandon, M. Topcu, Free vibration analysis of cracked beams by a combination of finite elements and component mode synthesis methods, Comput. Struct. 67 (1998) 215–223.
[6] E.I. Shifrin, R. Ruotolo, Natural frequencies of a beam with an arbitrary number of cracks, J. Sound Vib. 223 (1999) 409–423.
[7] M. Kisa, J.A. Brandon, Free vibration analysis of multiple open edge cracked beams by component mode synthesis, Struct. Eng. Mech. 10 (2000) 81–92.
[8] M. Kisa, J.A. Brandon, The effects of closure of cracks on the dynamics of a cracked cantilever beam, J. Sound Vib. 238 (2000) 1–18.
[9] E. Viola, L. Federici, L. Nobie, Detection of crack location using cracked beam element method for structural analysis, Theor. Appl. Fract. Mech. 36 (2001) 23–35.
[10] M. Krawczuk, Application of spectral beam finite element with a crack and iterative search technique for damage detection, Finite Elem. Anal. Des. 38 (2002) 537–548.
[11] D.P. Patil, S.K. Maiti, Detection of multiple cracks using frequency measurements, Eng. Fract. Mech. 70 (2003) 553–572.
[12] M. Kisa, Free vibration analysis of a cantilever composite beam with multiple cracks, Compos. Sci. Technol. 64 (2004) 1391–1402.
[13] M. Kisa, M.A. Gurel, Modal analysis of multi-cracked beams with circular cross section, Eng. Fract. Mech. 73 (2006) 963–977.
[14] P. Gudmundson, The dynamic behaviour of slender structures with cross-sectional cracks, J. Mech. Phys. Solids 31 (1983) 329–345.
[15] M.M.F. Yuen, A numerical study of the eigenparameters of a damaged cantilever, J. Sound Vib. 103 (1985) 301–310.
[16] P.F. Rizos, N. Aspragathos, A.D. Dimarogonas, Identification of crack location and magnitude in a cantilever beam from the vibration modes, J. Sound Vib. 138 (1990) 381–388.
[17] A.D. Dimarogonas, C.A. Papadopoulos, Vibrations of cracked shafts in bending, J. Sound Vib. 91 (1983) 583–593.
[18] C.A. Papadopoulos, A.D. Dimarogonas, Coupled longitudinal and bending vibrations of a rotating shaft with an open crack, J. Sound Vib. 117 (1987) 81–93.
[19] M.L. Kikidis, C.A. Papadopoulos, Slenderness ratio effect on cracked beam, J. Sound Vib. 155 (1992) 1–11.
[20] D.Y. Zheng, S.C. Fan, Vibration and stability of cracked hollow-sectional beams, J. Sound Vib. 267 (2003) 933–954.

[21] G.M. Dong, J. Chen, J. Zou, Parameter identification of a rotor with an open crack, Eur. J. Mech. A: Solids 23 (2004) 325–333.
[22] S.K. Jang, C.W. Bert, Free vibration of stepped beams: higher mode frequencies and effects of steps on frequency, J. Sound Vib. 132 (1989) 164–168.
[23] J.I. Wang, Vibration of stepped beams on elastic foundations, J. Sound Vib. 149 (1991) 315–322.
[24] J. Lee, L.A. Bergman, The vibration of stepped beams and rectangular plates by an elemental dynamic flexibility method, J. Sound Vib. 171 (1994) 617–640.
[25] H.P. Lee, T.Y. Ng, Vibration and buckling of a stepped beam, Appl. Acoust. 42 (1994) 257–266.
[26] M.A. De Rosa, P.M. Belles, M.J. Maurizi, Free vibrations of stepped beams with intermediate elastic supports, J. Sound Vib. 181 (1995) 905–910.
[27] S. Naguleswaran, Vibration and stability of an Euler–Bernoulli beam with up to three-step changes in cross-section and in axial force, Int. J. Mech. Sci. 45 (2003) 1563–1579.
[28] T.C. Tsai, Y.Z. Wang, Vibration analysis and diagnosis of a cracked shaft, J. Sound Vib. 192 (1996) 607–620.
[29] B.P. Nandwana, S.K. Maiti, Detection of the location and size of a crack in stepped cantilever beams based on measurements of natural frequencies, J. Sound Vib. 203 (1997) 435–446.
[30] T.D. Chaudhari, S.K. Maiti, Experimental verification of a method of detecting of cracks in taper and segmented beams based on modelling of transverse vibration, Int. J. Fract. 102 (2000) 33–38.
[31] Q.S. Li, Vibratory characteristics of multi-step beams with an arbitrary number of cracks and concentrated masses, Appl. Acoust. 62 (2001) 691–706.
[32] Q.S. Li, Free vibration analysis of non-uniform beams with an arbitrary number of cracks and concentrated masses, J. Sound Vib. 252 (2001) 509–525.
[33] O.N.L. Abraham, J.A. Brandon, The modelling of the opening and closure of a crack, J. Vib. Acoust. 117 (1995) 370–377.
[34] J.A. Brandon, O.N.L. Abraham, Counter-intuitive quasi-periodic motion in the autonomous vibration of cracked Timoshenko beams, J. Sound Vib. 185 (1995) 415–430.
[35] W.C. Hurty, Dynamic analysis of structures using substructure modes, AIAA J. 3 (1965) 678–685.
[36] G. Irwin, Fracture Mechanics, Structural Mechanics, Pergamon Press, 1960.
[37] H. Tada, P.C. Paris, G.R. Irwin, The Stress Analysis of Cracks Handbook, Paris Production Incorporated and Del Research Corporation, 1985.
[38] G.R. Cowper, The shear coefficient in Timoshenko's beam theory, J. Appl. Mech. (1966) 335–340.
[39] A.D. Dimarogonas, S.A. Paipetis, Analytical Methods in Rotor Dynamics, Applied Science Publishers., 1983.
[40] Z. Friedman, J.B. Kosmatka, An improved two-node Timoshenko beam finite element, Comput. Struct. 47 (1993) 473–481.
[41] C.A. Papadopoulos, A.D. Dimarogonas, Coupled longitudinal and bending vibrations of a cracked shaft, J. Vibr. Acous. Stress Rel. Des. 110 (1988) 1–8.